The Plant Cell, Vol. 16, 1263–1275, May 2004, www.plantcell.org © 2004 American Society of Plant Biologists

COTYLEDON VASCULAR PATTERN2–Mediated Inositol (1,4,5) Triphosphate Signal Transduction Is Essential for Closed Venation Patterns of Arabidopsis Foliar Organs

Francine M. Carland and Timothy Nelson[1]

Department of Molecular, Cellular, and Developmental Biology, Yale University, New Haven, Connecticut 06520-8104

Vein patterns in leaves and cotyledons form in a spatially regulated manner through the progressive recruitment of ground cells into vascular cell fate. To gain insight into venation patterning mechanisms, we have characterized the *cotyledon vascular pattern2* (*cvp2*) mutants, which exhibit an increase in free vein endings and a resulting open vein network. We cloned *CVP2* by a map-based cloning strategy and found that it encodes an inositol polyphosphate 5′ phosphatase (5PTase). 5PTases regulate inositol (1,4,5) triphosphate (IP_3) signal transduction by hydrolyzing IP_3 and thus terminate IP_3 signaling. *CVP2* gene expression is initially broad and then gradually restricted to incipient vascular cells in several developing organs. Consistent with the inferred enzymatic activity of *CVP2*, IP_3 levels are elevated in *cvp2* mutants. In addition, *cvp2* mutants exhibit hypersensitivity to the plant hormone abscisic acid. We propose that elevated IP_3 levels in *cvp2* mutants reduce ground cell recruitment into vascular cell fate, resulting in premature vein termination and, thus, in an open reticulum.

INTRODUCTION

Modern dicots have an interconnected vascular network that transports essential nutrients in a source-to-sink manner. This differs from the primitive vein pattern in which conducting tissue formed simple dendritic (tree-like) formations (Roth-Nebelsick et al., 2001). The closed reticulum pattern that characterizes the venation of dicot leaves is thought to have been derived from a primitive open conduit through positive selection because closed conduits have more efficient transport capacity and provide improved structure and stability to the leaf (Roth-Nebelsick et al., 2001).

During leaf development, veins form within a field of subepidermal ground cells in the form of procambium in an event that is developmentally coordinated with lamina formation (Dengler, 2001). Vein orders are formed progressively and join in a hierarchical manner (Telfer and Poethig, 1994; Nelson and Dengler, 1997; Kinsman and Pyke, 1998; Candela et al., 1999). The prominent midvein forms first, in parallel with the emerging leaf primordium and in continuity with vasculature of the central axis. Subsequently, secondary or lateral veins diverge from the midvein to extend toward leaf margins as the lamina expands laterally. As expansion continues, the minor veins, composed of tertiary, quaternary, and intramarginal veins, intercalate between and join the lower vein orders. Quaternary veins generally appear as freely terminating veinlets, defined as strands that are joined at only one end, presumably because ground cells have lost competence or signals for vascular cell fate. Before the differentiation of veins, their incipient paths can be recognized first as a path of ground cells with responsiveness of auxin-sensitive reporters (Mattsson et al., 2003) and then anatomically as files of elongated procambial cells that are visually distinct from ground cells. Several markers can identify procambial files, including Athb8, Athb20, and VH1 (Baima et al., 1995; Clay and Nelson, 2002; Kang and Dengler, 2002; Mattsson et al., 2003). The evident temporal and spatial coordination of procambial and mesophyll cell differentiation implicates continuous cell-to-cell communication along the path of vein recruitment and differentiation.

The directional transport of auxin appears to play a role in establishing the longitudinal polarity and strand continuity associated with vein formation (Sachs, 1991). The effects of exogenously applied auxin transport inhibitors and the pattern of activation of DR5 auxin-responsive reporter genes suggest that auxin acts as a positional cue for vein forming events (Mattsson et al., 1999, 2003; Sieburth, 1999). In addition, biochemical support for the polar flow of auxin is provided by the identification of the putative auxin efflux carriers, the asymmetrically localized PIN proteins (Galweiler et al., 1998). Venation pattern defects, such as loss of vascular cell polarity and of uniform cell files, are observed in mutants with defects in several auxin related genes. These mutants include those that were identified on the basis of defective embryo patterning, such as *monopteros*, *bodenlos*, and *gnom/emb30* (Berleth and Jurgens, 1993; Shevell et al., 1994; Busch et al., 1996; Przemeck et al., 1996; Hardtke and Berleth, 1998; Hamann et al., 1999, 2002), or of an alteration in auxin response such as *auxin resistant6* (Hobbie et al., 2000). Although the gene products of the vascular patterning mutants

[1] To whom correspondence should be addressed. E-mail timothy.nelson@yale.edu; fax 203-432-5632.

The author responsible for distribution of materials integral to the findings presented in this article in accordance with the policy described in the Instructions for Authors (www.plantcell.org) is: Timothy Nelson (timothy.nelson@yale.edu).

Article, publication date, and citation information can be found at www.plantcell.org/cgi/doi/10.1105/tpc.021030.

scarface (Deyholos et al., 2000) and *lopped1/tornado1* (Carland and McHale, 1996; Cnops et al., 2000) have not been identified yet, physiological analysis implicates aberrant auxin response or transport.

Other mutant studies imply roles for cytokinin (Mahonen et al., 2000; Inoue et al., 2001), small peptides (Casson et al., 2002), brassinosteroids (Szekeres et al., 1996; Choe et al., 1999), and sterols (Diener et al., 2000; Jang et al., 2000; Schrick et al., 2000, 2002; Carland et al., 2002; Souter et al., 2002) in vein patterns. There are phenotypic abnormalities shared between sterol and auxin mutants that include polarity defects in vascular cells and/or embryogenesis. It has been proposed that sterol defects influence the membrane localization of auxin carriers (Carland et al., 2002; Grebe et al., 2003), although the relationship between sterols and auxin-facilitated polarizing events has not been firmly established. Recently, *sterol methyltransferase1*^{orc} mutants were shown to have mislocalized PIN protein, providing a link between sterols and the auxin polarity maintaining machinery (Willemsen et al., 2003). Furthermore, *hydra* mutants exhibit enhanced auxin response (Souter et al., 2002).

The *cotyledon vascular pattern2* (*cvp2*) and *forked* (*fkd1*) mutants appear to end vascular strand propagation prematurely, resulting in an unclosed reticulum with open secondary and higher order veins (Carland et al., 1999; Steynen and Schultz, 2003). Both *cvp2* and *fkd1* mutants were isolated in genetic screens for vascular patterning mutants without obvious defects in plant growth or morphology. Neither mutant exhibits defects in vascular cell morphology or polarity, as do many of the auxin and sterol mutants described above. Although both mutants show a loss of vein anastomoses with many vein orders, they do show distinct differences. Consistent with the wild-type appearance of *cvp2*, no perturbations in auxin content, response, or transport were detected, and *cvp2* has an increase in cotyledon lateral veins. By contrast, *fkd1* exhibits reduced auxin response, an unaltered number of cotyledon lateral veins, and elongated first rosette leaves. Leaf morphological alterations are subtle in *fkd1* and absent in *cvp2*, supporting the hypothesis that the major veins influence leaf shape more than the minor veins do (Dengler and Kang, 2001). The characterization of *cvp2* mutants led us to postulate a role for *CVP2* in the perception or transduction of a signal critical for the propagation of procambial strand formation.

Here, we report that the vascular patterning gene *CVP2* encodes an inositol polyphosphate 5′ phosphatase (5PTase). 5PTases have been shown in animal systems (Majerus et al., 1999) and in plants (Berdy et al., 2001; Sanchez and Chua, 2001; Perera et al., 2002) to regulate inositol signal propagation by their ability to cleave a 5′ phosphate from various inositol stereoisomers. In this manner, they are negative regulators of inositol (1,4,5) triphosphate (IP_3) signal transduction and of other second messengers, such as Ca^{2+}. In agreement with the proposed role of 5PTases, we show that there are increased levels of IP_3 in *cvp2* mutants and that mutants are hypersensitive to abscisic acid (ABA). *CVP2* is expressed in developing vascular cells in several plant organs. *CVP2* is the only member of the 15 5PTases in *Arabidopsis thaliana* that has been identified by mutation. Its phenotype suggests a role for IP_3 signaling in an early stage of vascular patterning. We propose that the open vascular network in *cvp2* mutants is attributable to unregulated *CVP2*-mediated IP_3 production that elicits upregulation of otherwise tightly controlled response genes, presumably by the inappropriate release of Ca^{2+}. Misregulation of these genes prevents the specification of ground cells into vascular cell fate during vascular strand propagation.

RESULTS

cvp2 Mutants Have an Open Vein Network

A detailed description of the *cvp2* mutant phenotype was previously presented (Carland et al., 1999). Wild-type cotyledons have a closed reticulum generally consisting of three to four closed loops (Figure 1A). By contrast, *cvp2* mutant cotyledons exhibit an open reticulum, characterized by an increase in free vein endings (Figure 1B). Short stretches of veins, known as vascular islands because they appear to form in isolation from other veins, appear frequently in *cvp2* cotyledons. Unlike wild-type rosette leaves in which secondary veins join apical veins, in *cvp2* leaves, secondary veins usually do not meet previously formed veins distally (Figures 1C to 1F). This is particularly apparent with apical secondary veins. Wild-type tertiary veins bridge secondary veins to form a connected conduit. The corresponding tertiary veins in *cvp2* mutant leaves do not span secondary veins and appear to terminate prematurely. In contrast with wild-type quaternary veins, which form freely ending veinlets, the corresponding veins in *cvp2* mutant leaves appear as vascular islands and fail to form vein junctions. A comparison of wild-type and *cvp2* lateral vein development revealed that similar to wild-type veins, *cvp2* mutant veins show progressive decrease in girth but terminate prematurely (Carland et al., 1999), suggesting that *CVP2* promotes vascular cell proliferation and prevents premature vein termination.

Procambial Cell-Specific Expression of Athb8 Is Dependent on *CVP2* Function

To determine the stage at which *CVP2* acts in vein formation, we used the procambial cell-specific marker Athb8 (Baima et al., 1995; Kang and Dengler, 2002) as a reporter construct to monitor procambial cell patterning during embryogenesis because of the simplicity of the cotyledon venation pattern. A line with a single copy Athb8:β-glucuronidase (GUS) transgene was crossed to *cvp2* to generate a homozygous *cvp2*/Athb8:GUS line. Athb8:GUS staining was centrally localized, corresponding to future sites of vascular development, in both wild-type and *cvp2* heart and torpedo embryos, and was consistent with the unaffected midvein and root vasculature observed in *cvp2* seedlings (Figures 1G to 1J). In both wild-type and *cvp2* walking-stick stage embryos, Athb8:GUS was visible in the apical loop (Figures 1K and 1L). However, in the wild type, this loop was closed, and in *cvp2*, the open vein network was just beginning to appear. At the bent cotyledon stage of wild-type embryos, staining was restricted to procambial cells forming the four continuous loops observed in mature embryos and cotyledons (Figure 1M), whereas in *cvp2* embryos, staining revealed an open network, anticipating the vascular patterning defects observed in *cvp2* mutant cotyledons (Figure 1N). This confirmed our earlier

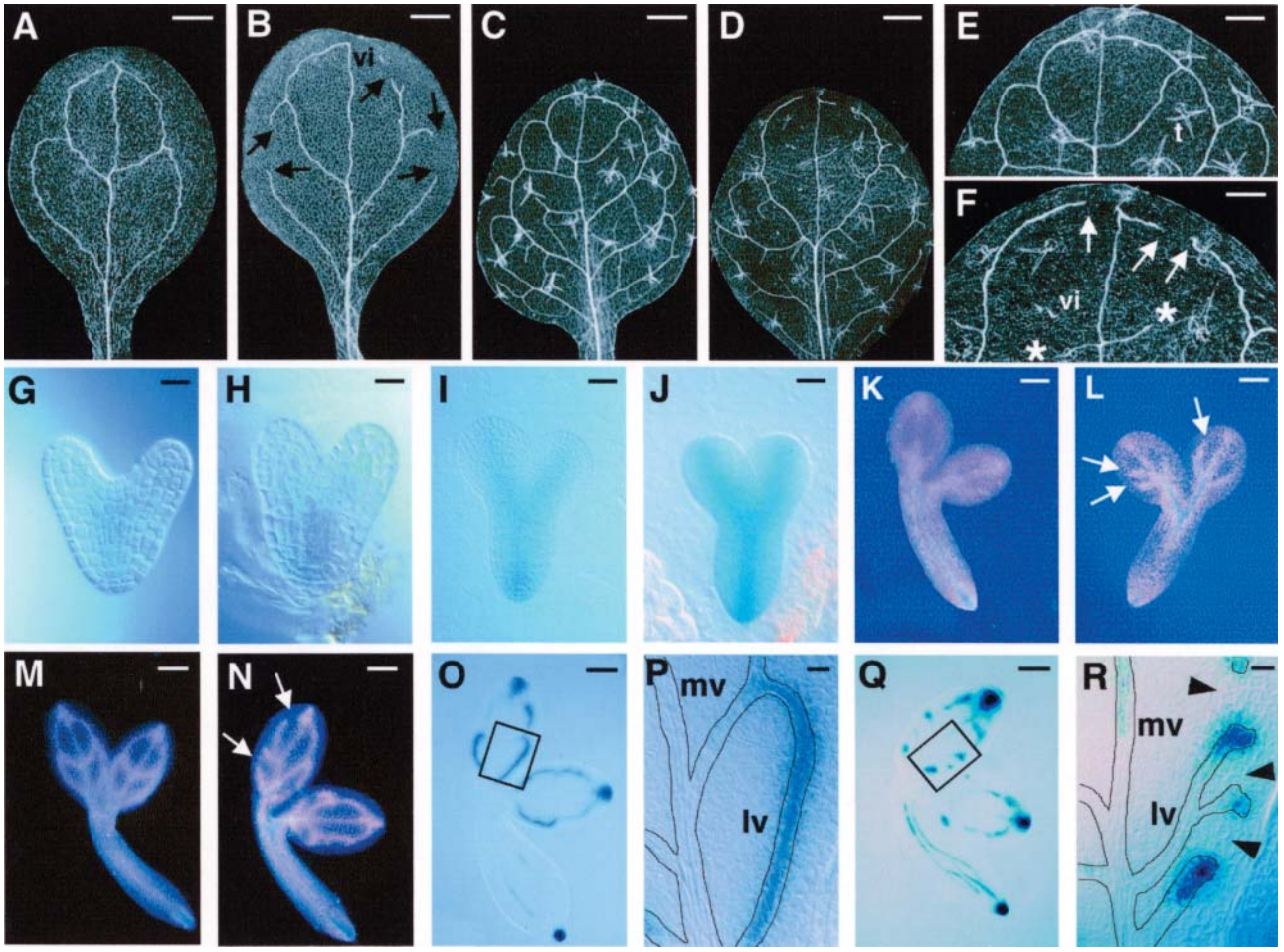

Figure 1. *CVP2* Acts Early in Procambial Patterning during Embryogenesis.

(A) to **(F)** Cleared specimens viewed with dark-field optics. Wild-type cotyledon **(A)**, *cvp2* cotyledon **(B)**, wild-type leaf **(C)**, and *cvp2* leaf **(D)** are shown. Higher magnification of **(C)** and **(D)** are shown in **(E)** and **(F)**, respectively. With dark-field optics, trichomes (t) appear translucent with three spikes.
(G) to **(N)** Athb8:GUS embryo expression. Wild-type heart **(G)**, *cvp2* heart **(H)**, wild-type torpedo **(I)**, *cvp2* torpedo **(J)**, wild-type walking stick **(K)**, *cvp2* walking stick **(L)**, wild-type bent cotyledon **(M)**, and *cvp2* bent cotyledon **(N)** are shown. Dark-field images are more sensitive than Nomarski optical images and show weak GUS expression as pink and strong GUS expression as blue.
(O) to **(R)** DR5:GUS expression of bent cotyledon stage embryo. Wild-type embryo **(O)**, wild-type proximal lateral vein at a higher magnification of the boxed region in **(O)** to show uniform DR5:GUS expression **(P)**, *cvp2* embryo **(Q)**, and *cvp2* proximal lateral vein at a higher magnification of the boxed region in **(Q)** to show short stretches of DR5:GUS expression in *cvp2* mutants **(R)**. Arrowheads designate absence of DR5:GUS. In wild-type embryos, 369 out of 394 lateral veins showed continuous DR5:GUS expression. In *cvp2* embryos, 33 out of 330 lateral veins showed continuous DR5:GUS expression. Roots of embryos in **(O)** and **(Q)** were distorted while separating cotyledons. Vein patterns are outlined in **(P)** and **(R)**.
Arrows indicate free vein endings of secondary veins; asterisks indicate free vein endings of tertiary veins. Dark-field optics were used for **(A)** to **(F)** and **(K)** to **(N)**; Nomarski optics were used for **(G)** to **(J)** and **(O)** to **(R)**. vi, vascular island; mv, midvein; lv, lateral vein. Bars = 500 μM in **(A)** to **(D)**, 250 μM in **(E)** and **(F)**, 10 μM in **(G)**, **(H)**, **(P)**, and **(R)**, 25 μM in **(I)** and **(J)**, 50 μM in **(K)** and **(L)**, and 80 μM in **(M)**, **(N)**, **(O)**, and **(Q)**.

observations of procambial cells in unstained embryos that *CVP2* was acting early in procambial strand formation during embryogenesis.

Procambial Cell Patterning in *cvp2* Mutant Embryos Is Coincident with DR5:GUS Expression

We used the DR5:GUS synthetic reporter construct (Ulmasov et al., 1997) to map auxin-responsive cells in *cvp2* mutant embryos. This auxin-responsive reporter has been used to infer local auxin levels (Sabatini et al., 1999) and can serve as an early indicator of preprocambial cell patterning during vein formation in developing leaves (Mattsson et al., 2003). DR5:GUS appeared in a progressively formed pattern that foreshadowed all vein orders as they appear in a developing leaf. To determine if the establishment of preprocambial formation was affected in *cvp2* mutant embryos, we generated a *cvp2*/DR5:GUS line and

examined DR5:GUS histochemical staining in embryos. The reporter gene was expressed in incipient vascular cells, before detectable vascular cell morphological changes, and was not expressed in fully elongated procambial cells, consistent with previous reports (Mattsson et al., 2003). As shown in Figures 1O and 1P, DR5:GUS marked secondary veins as a continuous file of cells in wild-type bent cotyledon stage embryos but was no longer expressed in the elongated procambial cells of the midvein. Distal secondary veins showed diminishing DR5:GUS expression as these cells elongated. Similar to the wild type, there was either no or very weak GUS histochemical staining in the elongated procambium of *cvp2* midvein and secondary veins (Figures 1Q and 1R). By contrast, *cvp2*/DR5:GUS mutant embryos at the same stage exhibited a discontinuous pattern characterized by short stretches of DR5:GUS-expressing cells that appeared to be vein termini. There was no evidence of DR5:GUS cells between these preprocambial foci, suggesting that *CVP2* acts before the acquisition of preprocambial identity (Figure 1R, arrowheads).

CVP2 Encodes a 5PTase

CVP2 was mapped to the top of chromosome one between the polymorphic markers F19P19 and PhyA (Figure 2A). Breakpoint analysis with flanking polymorphic markers, which we identified from known markers on the restriction fragment length polymorphism map or from the limited genomic sequence that was available at the time, localized *CVP2* to ~270 kb. Using probes derived from candidate BAC clones, we identified transformation-competent artificial clones (TAC) (Liu et al., 1999) that were within the *CVP2* region but did not span the *CVP2* region in its entirety. Positive TAC clones were introduced into the *cvp2* mutant, and because transgenic plants harboring full-length TAC clones failed to complement *cvp2*, we were able to further refine the map position of *CVP2* to overlapping BACs T25N20 and F3F20. Additional potential *CVP2*-containing clones derived from a BAC F3F20 library and a binary cosmid library (Schulz et al., 1994) that were assayed for *cvp2* complementation failed to rescue *cvp2*. There were four annotated genes in the *CVP2* region that were not represented in those libraries, including T25N20.12, which was mutant in *cvp2-1*. Sequencing of the *cvp2-1* allele of gene T25N20.12 revealed a single nucleotide substitution in the gene encoding a previously uncharacterized 5PTase (At1g05470; Figure 2B). Phenotypic analysis of six *cvp2* alleles (*cvp2-1* through *cvp2-6*) showed that all mutant alleles had identical phenotypes, suggesting that they represented null alleles. Sequence analysis of four alleles (*cvp2-1*, *cvp2-2*, *cvp2-3*, and *cvp2-4*) revealed single nucleotide changes consistent with the production of a nonfunctional protein (Figure 2B).

There were discrepancies in the exon/intron annotation of *CVP2*, which is based on software predictions because the *CVP2* cDNA had not been identified. The observation that a *CVP2* cDNA is not represented in the collection of 140,000 ESTs suggested that *CVP2* is a rare message. In agreement with this low level of expression, we were unable to detect a *CVP2* transcript by RNA gel blot hybridization using 10 μg of RNA from various organs and from hormonal-induced (cytokinin, ethylene, brassinosteroid, auxin, and gibberellic acid) seedlings (data not shown). Furthermore, attempts to amplify full-length *CVP2* cDNA by RT-PCR using RNA templates from various wild-type tissues failed. To identify the *CVP2* cDNA, we conducted RT-PCR using transgenic seedlings overexpressing the *CVP2* genomic clone as template RNA. Nested PCR resulted in an amplified product of 1.83 kb. Sequencing of this cDNA, which encodes a 609–amino acid protein, revealed the exon/intron structure displayed by the National Center for Biotechnology Information (NCBI) (Figure 2B). *CVP2* identity was verified upon full complementation of the *cvp2* vascular patterning defect with a genomic clone encompassing the coding region and flanking 1.5 kb upstream region (Figure 2C), although overexpression of *CVP2* cDNA or of a genomic clone with the 35S promoter of *Cauliflower mosaic virus* did not rescue *cvp2* vein patterns, indicating sensitivity to 5PTase levels. Overexpression of *CVP2* cDNA or of a genomic clone in the wild type did not yield a vascular patterning defect.

5PTases cleave the phosphate in the 5′ ring position of the water-soluble I(1,4,5)-P_3 and I(1,3,4,5)-P_4 and/or the lipids PI(4,5)-P_2 and PI(3,4,5)-P_3 (Majerus et al., 1999). In mammalian systems, 5PTases are classified into four groups (Types I, II, III, and IV) based on sequence homology and substrate specificity that is usually dependent upon the 5PTase subcellular localization (Matzaris et al., 1998; Majerus et al., 1999). For example, the cytosolic/peripheral membrane phosphoinositide phosphatases, the synaptojanins, hydrolyze both soluble and insoluble substrates and are classified as Type II 5PTases. Computer analysis suggested that only Type I and Type II 5PTases are represented in Arabidopsis, maize (*Zea mays*), rice (*Oryza sativa*), tomato (*Lycopersicon esculentum*), and *Medicago truncatula* (Berdy et al., 2001). Phylogenetic analysis positioned *CVP2* and eight other At5PTases as Type I (Berdy et al., 2001), which in mammalian systems have been shown to be the most active 5PTases (Majerus et al., 1999). Mammalian Type I 5PTases hydrolyze IP_3 and IP_4, and because IP_3 allows the release of internally stored Ca^{2+}, they are hypothesized to terminate Ca^{2+} signaling (Connolly et al., 1985). Both At5PTase1 and At5PTase2 have been shown to use IP_3 and IP_4 as substrates (Berdy et al., 2001; Sanchez and Chua, 2001). At5PTase1 is unable to hydrolyze the lipid-linked inositol phospholipids, thus confirming its identity as Type I 5PTase (Berdy et al., 2001). Like all 5PTases, *CVP2* contains the conserved domains I and II (Connolly et al., 1985). *CVP2* is closely related to two other Arabidopsis 5PTases, At2g32010 and At3g63240, sharing 72 and 52% identities, respectively (Figure 3A). Homology of *CVP2* to other Type I At5PTases drops off dramatically to 30 to 36% identities. In this regard, it is significant that a monocot rice 5PTase is more closely related to *CVP2* than *CVP2* is to other At5PTases.

The x-ray crystal structure of Type II 5PTase synaptojanin from *Schizosaccharomyces pombe* revealed an endonuclease fold originally identified in DNase I (Tsujishita et al., 2001). Protein alignment software showed that Types I and II 5PTases, including *CVP2*, src homology2 (SH2)-containing inositol phosphates, and other proteins involved in diverse signaling pathways, have a structural similarity to Mg^{2+}-dependent endonucleases (Figure 3B) through the conservation of catalytic residues and a four-layered α/β sandwich motif that is a structural domain with two predominantly antiparallel sheets positioned between two α-helical layers (Dlakic, 2000). Other members of the

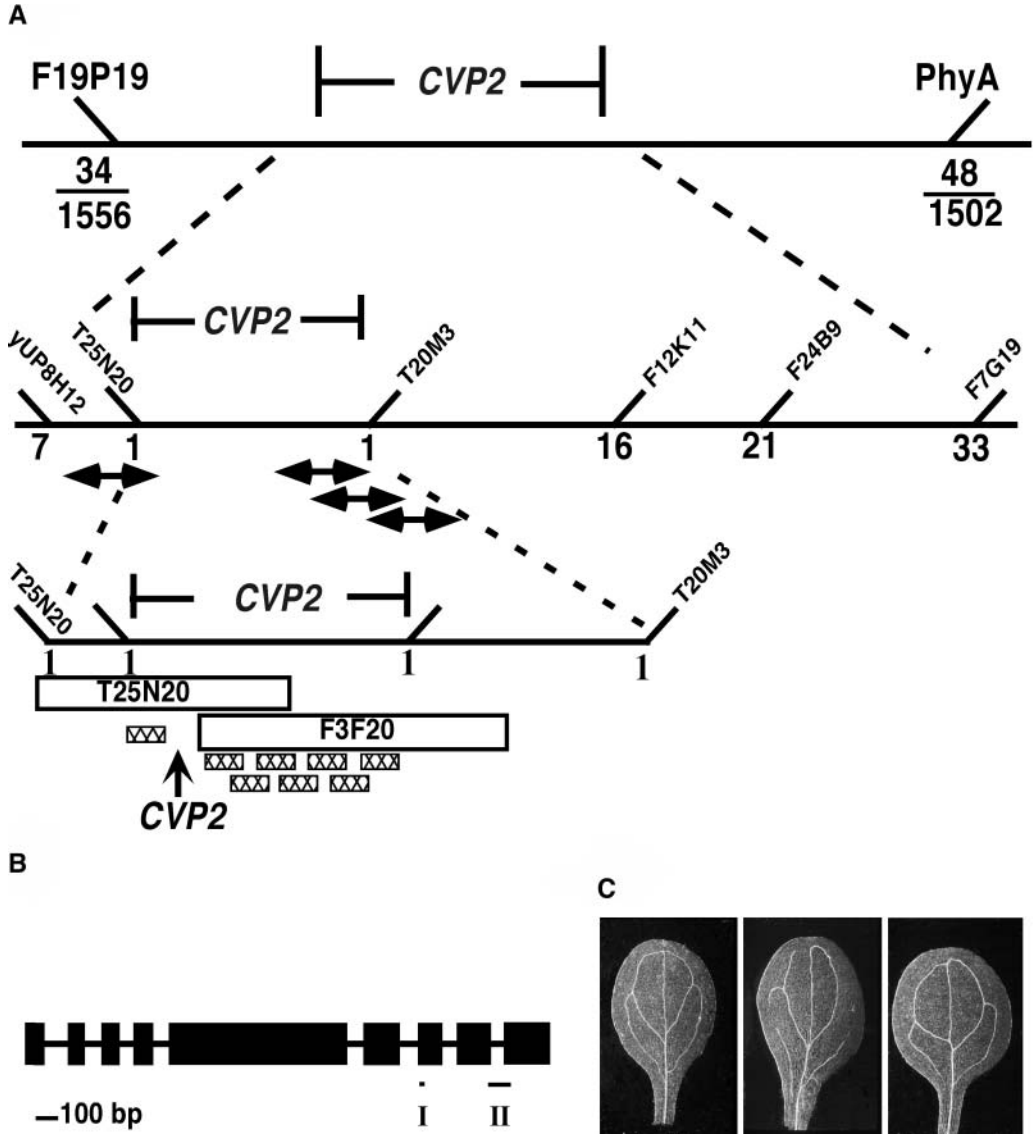

Figure 2. Map-Based Cloning of *CVP2.*

(A) Scheme showing the map-based cloning of *CVP2*. *CVP2* was localized to the top of chromosome one, represented by a solid horizontal line, using the flanking markers PhyA and F19P19. For PhyA and F19P19, the fractions indicate the number of recombinants over the total number of meiotic events. The numbers of recombinants for additional markers are shown below the diagonal line. The name of the BAC clone (45° angle) is given for a specific polymorphic marker that was derived from the BAC. Double-headed arrows represent TACs that were identified in the region by hybridization studies. Hatched boxes represent some of the clones that were found to reside in the vicinity of *CVP2* and assayed for *cvp2* complementation. Because none of these clones rescued the *cvp2* mutant phenotype, *CVP2* was localized to one of four genes on BAC T25N20 that were not represented in the libraries.

(B) *CVP2* gene structure. Solid vertical bars represent exons. Exon/intron junctions were determined by comparing a *CVP2* cDNA isolated from seedling tissue with the genomic sequence in the database. Mutations identified in four *cvp2* alleles are given. Specifically, *cvp2-1* has a G-to-A nucleotide substitution that substitutes a Gly residue for Asp at amino acid 567; *cvp2-2* contains a C-to-T nucleotide substitution that changes an Ala to a Val in the PAWCDRIL (amino acid 535) site of domain II; *cvp2-3* contains a G-to-A nucleotide substitution that changes a Trp to a stop codon at amino acid 144; *cvp2-4* (diepoxybutane mutant) has an A-to-T nucleotide substitution at the fourth exon/intron junction (amino acid 136), which is predicted to cause a splicing error resulting in a misread message for 45 residues before termination. Short horizontal bars represent 5PTase signature motifs, domains I and II.

(C) Complementation of *cvp2* with 5PTase. A genomic clone of At1g05470 containing the coding region and 1.5 kb upstream of the translational start codon was introduced into *cvp2-1* mutants. Cleared specimens were viewed with dark-field optics. Left, the wild type; center, *cvp2-1*; right, *cvp2-1*/At1g05470.

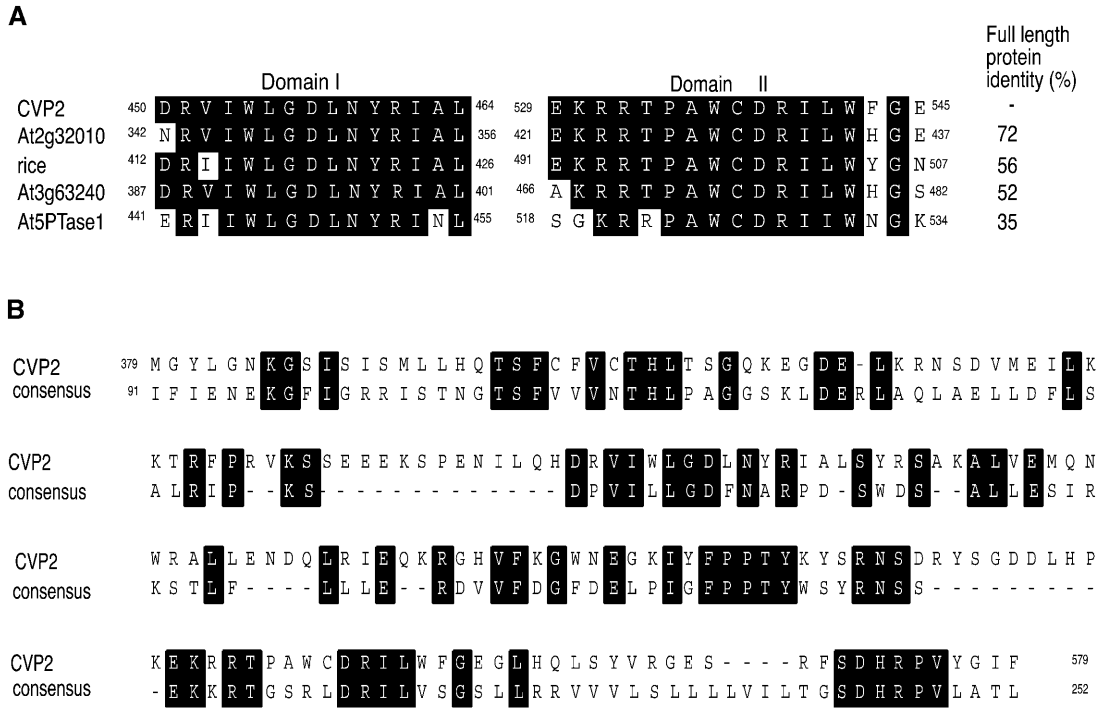

Figure 3. *CVP2* Is a Member of the Endonuclease/Exonuclease/Phosphatase Family.

(A) Alignment of *CVP2* with other plant 5PTases. The accession number for the rice 5PTase is AA037964.

(B) *CVP2* is aligned to a consensus sequence for endonuclease/exonuclease/phosphatase family members according to the NCBI conserved domain database (http://www.ncbi.nlm.nih.gov/Structure/cdd). The C-terminal part of the CVP2 protein is shown. Members with accession numbers for which the consensus sequence was derived include the following: *S. pombe* synaptojanin, 1I9Y_A; leptospira hemolytic protein, AAB68647; *S. pombe* RNA nuclease, CAB42372; *C. elegans* reverse transcriptase, CAB07490; catabolite repressor protein, ACC44428; *Homo sapiens* Type I 5PTase, Q14642; bovine DNase I, 1DNK_A; *Escherichia coli* Exonuclease III, 1AKO; and human endonuclease I 1DEB_B. Alignments were conducted using MacVector 7.0 (Oxford Molecular, Madison, WI). Identical residues are shaded black.

endonuclease/exonuclease/phosphatase family include major human apurinic/apyrimidinic endonuclease, yeast carbon catabolite repressor protein, which is involved in transcriptional activation and cell cycle regulation, and cytolethal distending toxin B, which causes cell cycle arrest (Dlakic, 2000). The presence of the nuclease catalytic core suggests that this diverse class of proteins has similar cleavage mechanisms but distinct substrate specificity.

CVP2 Is Expressed in Developing Vascular Cells of Many Different Organs

cvp2 mutations affect the vascular pattern of all foliar organs (Carland et al., 1999), suggesting that *CVP2* is required in numerous organs. Because *CVP2* was expressed at low levels, we examined its expression pattern throughout development using GUS reporter gene expression (see Methods). During early stages of embryogenesis, CVP2:GUS was broadly expressed throughout globular and early torpedo stages (Figures 4A and 4B). At the late torpedo stage, CVP2:GUS was strongly expressed in developing vascular cells and weakly expressed in surrounding cells (Figure 4C). By the walking-stick stage, CVP2:GUS was restricted to incipient vascular cells that delineated the apical loop and midvein of the cotyledon and root vasculature (Figure 4D). A similar pattern was observed during leaf development (Figures 4E to 4H). CVP2:GUS was strongly expressed in procambium and weakly expressed in areole cells in emerging leaves (Figures 4E and 4F). As leaves continued to expand, CVP2:GUS was limited to developing vascular cells (Figures 4G and 4H). Procambium-specific CVP2:GUS histochemical staining extended in parallel with the elongating root (Figures 4I and 4J) until root maturity, when CVP2:GUS was localized to two immature vascular cell files flanking the central core in the root differentiation zone (Figures 4K and 4L). During inflorescence development, CVP2:GUS expression was broad in young floral buds and gradually became restricted to the procambium of cauline leaves, sepals, petals, gynoecia, and anthers (Figures 4M to 4P). In summary, diminishing CVP2:GUS expression occurs in conjunction with vascular cell fate determination in developing organs.

CVP2 Has Elevated IP_3 Levels and Increased Sensitivity to ABA

Transgenic manipulation of 5PTase levels alters IP_3 levels (Berdy et al., 2001; Sanchez and Chua, 2001; Perera et al., 2002). If

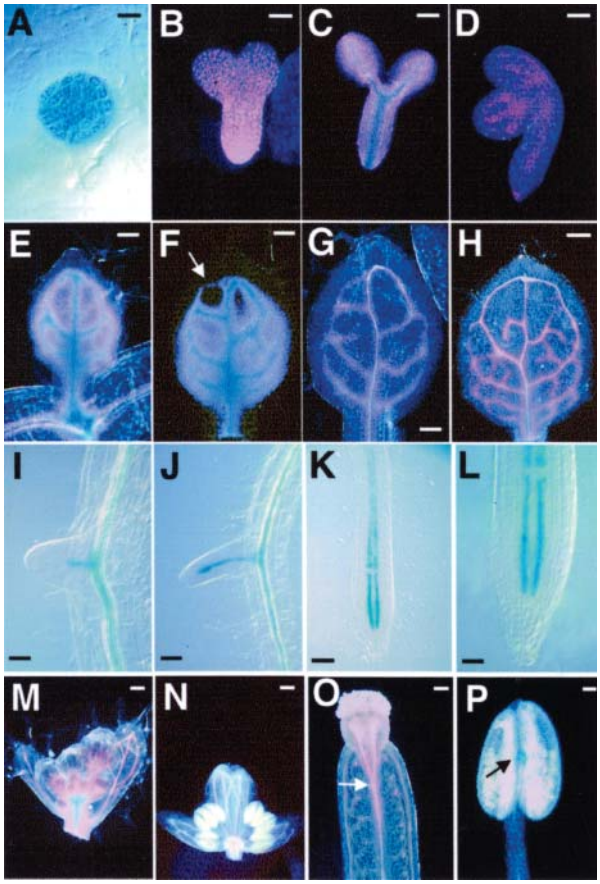

Figure 4. *CVP2* Expression by GUS Histochemical Staining.

(A) to **(D)** Embryos at globular **(A)**, torpedo **(B)**, late torpedo **(C)**, and walking-stick stages **(D)**.

(E) to **(H)** Sequential series of developing first rosette leaf.

(E) Young leaf to show strong *CVP2* expression in procambial cells and weaker expression in areoles.

(F) Slightly more mature leaf to show the decrease in weak areole *CVP2* expression at leaf apex (arrow) reflecting the basipetal maturation of the leaf.

(G) More advanced leaf that demonstrates *CVP2* expression in all developing veins.

(H) *CVP2* expression is restricted to developing veins in fully developed leaf. Note the absence of GUS staining in the apical loop in which vascular cells have already differentiated as tracheary elements and appear as white cells.

(I) to **(L)** Root expression.

(I) and **(J)** *CVP2* is expressed in the procambial core of the emerging lateral root.

(K) and **(L)** *CVP2* expression is limited to root tip, specifically to two procambial cell files.

(M) to **(P)** Floral expression of *CVP2*. *CVP2* is broadly expressed in inflorescence **(M)** and then restricted to developing floral organ veins, such as those in the sepal **(N)**, gynoecium **(O)**, and anther **(P)**.

Dark-field optics were used for **(B)** to **(H)** and **(M)** to **(P)**; Nomarski optics were used for **(A)** and **(I)** to **(L)**. Bars = 10 μM in **(A)**, 25 μM in **(B)**, **(I)**, and **(L)**, 40 μM in **(C)**, 50 μM in **(D)**, **(E)**, **(F)**, **(J)**, **(K)**, and **(P)**, 60 μM in **(G)**, 100 μM in **(H)**, **(M)**, and **(O)**, and 200 μM in **(N)**.

CVP2 is regulating IP_3 levels, then one would anticipate higher IP_3 levels in *cvp2* mutants because IP_3 would not be hydrolyzed to the inactive form inositol (1,4) diphosphate (IP_2). Measurement of IP_3 levels showed greater than a threefold increase in *cvp2-1* seedlings compared with the wild type (Figure 5). Modulation of IP_3 levels has been shown to affect ABA signaling. Transgenic plants overexpressing At5PTase I and II both showed ABA insensitivity (Sanchez and Chua, 2001; Burnette et al., 2003). Similarly, loss-of-function mutations in the *FIERY1* (*FRY1*) gene, an inositol polyphosphate 1-phosphatase that shows low level IP_3 catabolism, exhibits ABA hypersensitivity that is associated with elevated IP_3 levels (Xiong et al., 2001). To address ABA response in *cvp2*, dose–response experiments were conducted, measuring seed germination as a function of ABA level (Figures 6A and 6B). On media with no hormone, wild-type and *cvp2* germination rates were indistinguishable, suggesting that *cvp2* is not sensitive to endogenous ABA levels. On ABA-containing media, *cvp2* showed lower levels of seed germination compared with the wild type, indicating hypersensitivity to exogenous ABA. *cvp2* root growth also showed increased sensitivity to ABA. After 4 d of growth on 10 μM ABA, wild-type root growth was 41 ± 2.4% inhibited. However, *cvp2* root growth was inhibited by 56 ± 4.3%. In contrast with *fry1*, which exhibited elevated responses to additional stresses, such as high osmotic levels, *cvp2* seedlings appeared to demonstrate wild-type responses to NaCl and mannitol (data not shown), suggesting that aberrant *cvp2* IP_3 signaling specifically affects ABA response rather than a general stress response.

DISCUSSION

Dicots have a vascular pattern composed of reiterating vein branching. The mechanisms that guide this developmental process are not well understood. We previously reported on the *cvp2* mutant, which is characterized by a reduction in cell

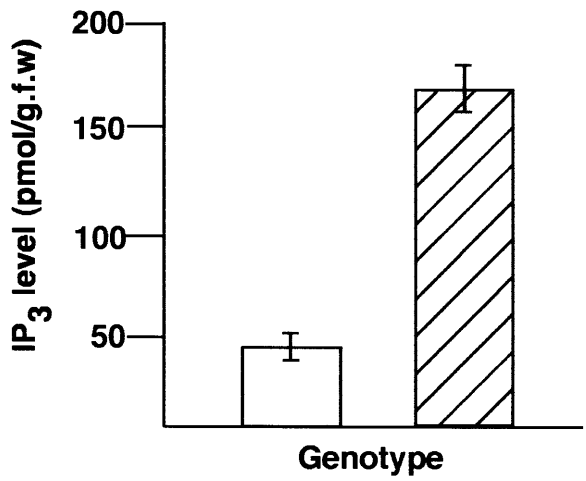

Figure 5. IP_3 Levels Are Elevated in *cvp2* Mutants.

Experiments were done in triplicate and error bars indicate standard error. Open, the wild type; hatched, *cvp2*. g.f.w., grams of fresh weight.

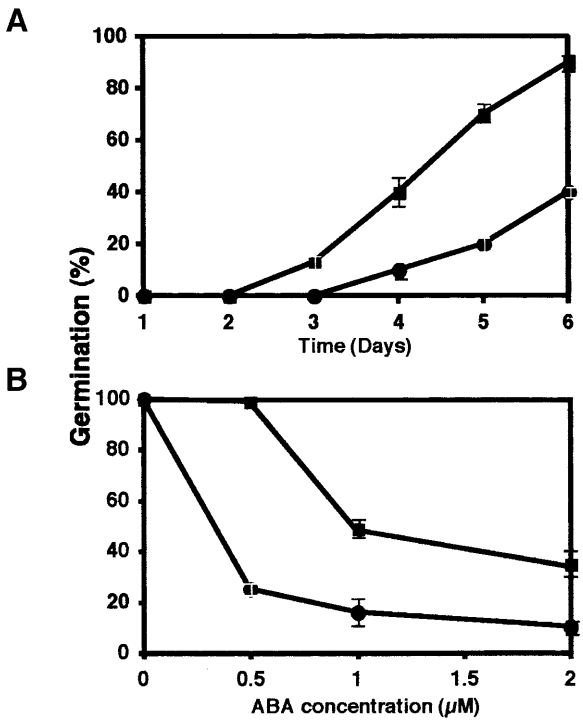

Figure 6. *cvp2* Response to ABA.

Seed germination was measured on increasing doses of ABA for 6 d. Wild-type and *cvp2* seed germination on 2 μM ABA over a 6-d period **(A)** and on day 4 with increasing amounts of ABA **(B)**. Squares, the wild type; circles, *cvp2*. Values represent triplicate experiments, and error bars show standard error.

recruitment into vascular tissue but otherwise normal vascular cell morphology. Consistent with its wild-type appearance, *cvp2* exhibits no defects in auxin biosynthesis, response, or transport. Based on our characterization, we postulated an early role for *CVP2* in the perception or transduction of a signal that regulates vascular strand propagation. Mutations in the 5PTase encoded by *CVP2* result in higher IP_3 levels and revert the normally closed reticulum of Arabidopsis to a more primitive open reticulum. *CVP2* represents the only member of this gene family identified by mutation. This finding provides the first evidence of a role for the highly conserved signal transduction pathway, IP_3 signaling, in vascular patterning.

IP_3-Facilitated Release of Calcium Transients and Development

In mammalian systems, IP_3-mediated Ca^{2+} influx, controlled by 5PTases, is involved in diverse cellular processes, such as regulation of gene transcription, secretion, ovulation, cytoskeletal rearrangements, and cell cycle (Berridge, 1993, 1995). As has been shown in animal and plant systems, cells respond to oscillations in Ca^{2+} that are differentially perceived and spatially restricted. Type I 5PTases, which use IP_3 and IP_4 as substrates, are primary regulators of IP_3-facilitated Ca^{2+} release (Speed et al., 1996). For example, the underexpression of a Type I 5PTase by antisense methods in rat kidney cells failed to terminate IP_3 signaling events and resulted in the spontaneous release of Ca^{2+} without external stimulation. A 2.6-fold increase in IP_3 was associated with a 4.1-fold increase in basal intracellular Ca^{2+} and resulted in transformed cells characterized by more rapid growth and the ability to form colonies on soft agar and tumors in nude mice (Speed et al., 1999). On the organismal level, a distinct number of calcium oscillations regulates the egg-to-embryo transition in mice (Ducibella et al., 2002). Initiation of transition requires the fewest Ca^{2+} transients, and progression requires prolonged exposure to Ca^{2+} transients. In plants, there are established Ca^{2+} parameter-regulated developmental processes exemplified by stomatal closure. A specific Ca^{2+} signature with a defined frequency of Ca^{2+} oscillations controls the amount of stomatal closure, such that an increase or decrease in the frequency of Ca^{2+} oscillations prevents stomatal closure (Allen et al., 2001). In this manner, a single signaling molecule can drive multiple events by the specific Ca^{2+} requirement of the process (Berridge et al., 2003).

CVP2-Mediated IP_3 Signal Transduction Regulates Vein Patterns

Based on the role of animal 5PTases to act as second messengers and regulate incremental Ca^{2+} release in response to a primary stimulus (Berridge, 1993), we propose a revised model specific for the involvement of *CVP2* in IP_3-regulated vascular patterning (Figure 7A). A membrane-bound receptor perceives a primary stimulus and triggers a G protein–linked phospholipase C to cleave the phospholipid, phosphotidylinositol (4,5) bisphosphate (PIP_2), into diacylglycerol and IP_3. IP_3 releases Ca^{2+} from internal stores in a tightly controlled manner to elicit the initialization of ground cells into vascular cells. *CVP2* acts as a negative regulator of IP_3 signaling by hydrolyzing IP_3 into the inactive form IP_2. During the extension of wild-type procambial strands, *CVP2* regulates IP_3 levels and the release of Ca^{2+}, instructing ground cells to acquire vascular cell identity (Figure 7B). In *cvp2* mutants, the absence of functional *CVP2* causes excessive IP_3 signaling, leading to persistent Ca^{2+} release, possibly without oscillations, and to an aberrant response, thereby reducing the number of ground-to-procambial cell transitions. This scenario is analagous to events during stomatal closure in which Ca^{2+} is required for stomatal closure; however, persistent Ca^{2+} exposure disrupts stomatal movement. This defect is restricted to vascular cell proliferation (vein girth) and continuity (vein length) and thus does not affect vein initiation in most vein orders, suggesting that *CVP2* is not the limiting factor in vein development. We propose that wild-type veinlet formation, whose vein endings normally terminate in the areole, show a similar *cvp2* Ca^{2+} response profile. The use of Ca^{2+} imaging tools, such as chameleon indicators, will enable us to visualize elevated Ca^{2+} levels at the cellular level.

How might misregulated *cvp2* response genes result in an open reticulum? One possibility is that *cvp2* Ca^{2+} response prevents the stimulation of Ca^{2+}-dependent effectors to act as cell-to-cell communicators for ground-to-procambial cell transition. An alternative model is based on the role of members of

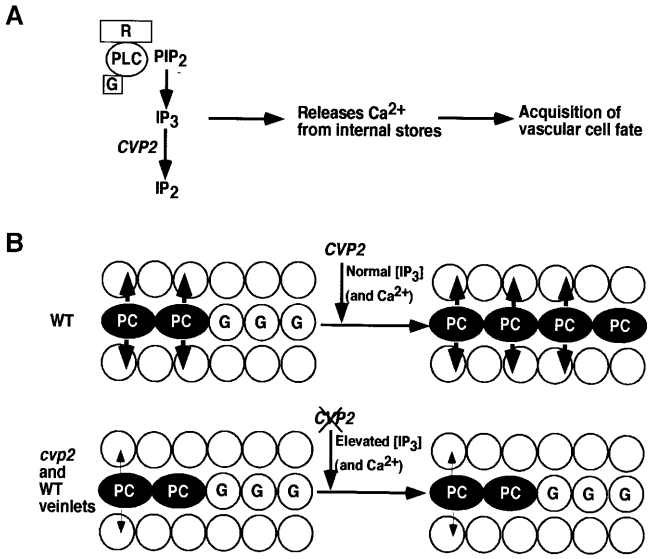

Figure 7. Model for the Role of *CVP2*.

(A) Hydrolyzing activity of *CVP2*. This model is based on animal systems in which the role of 5PTases is better understood. In response to as yet unidentified external stimulus, a membrane receptor activates phospholipase C (PLC)/G protein complexes (G) to breakdown PIP_2 into IP_3 (and diacylgylcerol). Acting as a second messenger, IP_3 amplifies the primary signal by releasing Ca^{2+} from internal stores. The downstream biological response for the appropriate Ca^{2+} parameters is acquisition of vascular cell fate. *CVP2* serves to hydrolyze IP_3 into the inactive form, inositol (1,4) diphosphate (IP_2), and thus terminates IP_3 signal transduction.

(B) Progessing procambial strand (PC) encounters ground cells (G). In the wild type, *CVP2* would act to prevent sustained Ca^{2+} oscillations by hydrolyzing IP_3 into IP_2. In this manner, the correct Ca^{2+} signature is perceived by downstream Ca^{2+}-dependent target genes, resulting in the recruitment of ground cells into vascular cell fate. In *cvp2* foliar organs and in freely terminating wild-type veinlets, because of the absence of *CVP2* hydrolytic activity, IP_3 levels are elevated, resulting in sustained Ca^{2+} release. The inappropriate Ca^{2+} levels reduce ground cell specification into procambial cells, presumably by misregulated Ca^{2+} response genes, and the veins prematurely terminate. The decrease in size and number of arrows from the procambial cells indicates that the radial proliferation of *cvp2* veins is also affected.

the endonuclease/exonuclease/phosphatase family in other systems as cell cycle regulators. In *cvp2* developing veins, ground cells lose vascular cell competence before completion of all vein orders formed during leaf development. In *cvp2* mutants, excessive Ca^{2+} release may cause aberrant cell cycling, resulting in either accelerated lamina differentiation or delayed procambial strand formation, in either case affecting the competence of cells to respond to inductive signals. The use of well-defined procambial and cell cycle markers will assist in distinguishing these possibilities. These models are based on the novel role of IP_3 signaling in vascular patterning and are in agreement with *CVP2* acting independently from other vascular patterning genes.

There are two models proposed for venation patterns. One model, the diffusion-reaction prepattern hypothesis, proposes that an initially homogenous field can be patterned by the interplay between a long-range diffusible inhibitor and an autocatalytic molecule (Meinhardt, 1996). The second model, known as the canalization of signal flow hypothesis, proposes that the patterning of aligned, polar vascular cells is a consequence of the directional flow of auxin (Sachs, 1991). The finding that the open reticulum formed in *cvp2* is because of impaired IP_3 signal transduction neither supports nor refutes either model. Basing the phenotype on the diffusion-reaction model, elevated IP_3 levels and its subsequent effectors in *cvp2* may act antagonistically with the reinforcing mechanism or synergistically with the inhibitor. With regards to the canalization model, auxin may not be able to be transported from one *cvp2* procambial cell to an adjacent cell because of defective transport capacity as a result of elevated IP_3 signaling. However, auxin itself has been reported to rapidly induce IP_3 signaling (Ettlinger and Lehle, 1988). Furthermore, unlike many other venation patterning mutants, *cvp2* mutants exhibit no auxin-associated defects, and based on double mutant combinations, appear to act independently from mutants with auxin-related vascular patterning defects, such as *cvp1* (Carland et al., 1999) and *monopteros* (F. Carland and T. Nelson, unpublished data). Elucidating the *cvp2* open vein network awaits the identification of additional components in *CVP2*-mediated IP_3 signal transduction.

The venation patterns of all foliar organs are affected in *cvp2* mutants, corresponding to the *CVP2* expression pattern. However, *CVP2* is also expressed in the root, which is unperturbed in *cvp2* mutants. This exception may be attributable to redundancy with the two closely related At5PTases that also show root expression (F. Carland and T. Nelson, unpublished data). Analysis of *CVP2* promoter-driven At5PTases and double mutant analysis should reveal overlapping functions among the At5PTases. Alternatively, because *CVP2* disruption appears to only affect vein continuity in lateral vein orders, it is possible that the root vasculature would not show a phenotype as a result of different regulation than that observed in foliar organs because root vasculature is maintained by fixed cell files and not reticulated. This may be analogous to the midvein of foliar organs, which is also unaffected in *cvp2* mutants. In light of this result, it is interesting that the monocot rice, which has parallel vein patterns, has a 5PTase closely related to *CVP2*. In fact, *CVP2* shares more identities to this rice 5PTase than to most of the other Arabidopsis 5PTases. It is tempting to speculate a role for this 5PTase in the extension of transverse veins in monocot leaves. Similar to *cvp2*, the rice mutant *radicleless1* exhibits premature termination of commissural veins, but in contrast with *cvp2* mutants, it is also affected in auxin response (Scarpella et al., 2003).

cvp2 represents the only reported mutation in the At5PTases. Only null mutants were identified, suggesting that weaker alleles do not have a detectable phenotype. The only other mutation reported in a Type I 5PTase in an intact organism is in *Caenorhabditis elegans* (Bui and Sternberg, 2002). The targeted deletion of a Type I 5PTase in *C. elegans* resulted in a developmental abnormality causing aberrent ovulation, suggesting that this 5PTase is a negative regulator of IP_3 signaling required during ovulation. However, the misexpression of *C. elegans*

Type I 5PTase did not cause a phenotype. Similarly, the gain-of-function version of *CVP2* did not affect vascular patterning in the wild type or in *cvp2* mutants. Misexpression of *CVP2* and *CVP2*-like genes by inducible promoters or cell-specific promoters may yield additional information on the phenotype of reduced IP_3 levels predicted by the role of *CVP2* as a negative regulator of IP_3 signaling.

IP_3 Signaling and ABA Response

Several genes have been implicated in ABA response, including those involved in small ubiquitin-like modifier conjugation, farnesylation, signaling, and stress response (Cutler et al., 1996; Pei et al., 1998; Xiong et al., 2001; Jung et al., 2002; Kwak et al., 2002; Lois et al., 2003). In many but certainly not all cases, gain-of-function versions of ABA response genes, either through mutation or through overexpression, exhibited insensitivity to ABA, and conversely, recessive alleles demonstrated increased sensitivity to ABA. For example, dominant *ABA insensitve1* (*abi1*) mutants showed resistance to ABA, whereas loss-of-function *abi1* alleles are hypersensitive to ABA (Gosti et al., 1999). IP_3 regulators have also been shown to exhibit similar profiles in ABA response. *FRY1*/*SAL1* encodes a bifunctional protein with inositol polyphosphate 1-phosphatase and 3′(2′),5′ bisphosphate nucleotidase activities (Murguia et al., 1995; Quintero et al., 1996; Xiong et al., 2001). Further testing of substrate specificity also suggested a role for *FRY1* in hydrolyzing IP_3, and indeed, *fry1* plants had elevated IP_3 levels (Xiong et al., 2001). *fry1* mutants were also hypersensitive to ABA and showed elevated activation of several ABA- and stress-responsive genes. Experiments directed at transgenic manipulation of 5PTases in plants included dexamethasone-induced overexpression of At5PTase II and overexpression of human Type I 5PTase and At5PTase I (Berdy et al., 2001; Sanchez and Chua, 2001; Perera et al., 2002). In the cases tested, elevated levels of 5PTase resulted in decreased IP_3 levels and in ABA insensitivity. In the case of human Type I 5PTase overexpression, PIP_2 levels were also reduced. Misexpression of the ABA-induced At5PTase I caused a delay in additional ABA-induced genes (Burnette et al., 2003). These results suggested that At5PTase I acts to terminate ABA signaling. There were no reports of vein pattern defects in the *fry1* or At5PTase overexpressors, and at this time, the causal relationship between *CVP2*-regulated ABA signaling and venation patterns is unclear, but the altered ABA response in *cvp2* mutants is consistent with other members of IP_3 regulators.

Angiosperms have a closed reticulum that is thought to have arisen from the primitive open vein network for redundancy in transport in case of plant injury and for more efficient transport (Roth-Nebelsick et al., 2001). Freely ending veinlets may be the remnants of this open reticulum that are now confined to higher vein orders. We speculate that IP_3 signaling played a role in evolution of open to closed vascular networks, although it may not be the primary determinant because of the second messenger role. The principal regulator of a closed reticulum may be the stimulus that is perceived. Using *CVP2* as a reference point, we can proceed to identify downstream targets through microarray technology and in reverse to elucidate the upstream components. For example, *CVP2* itself is likely to be tightly regulated based on the rareness of message and on the highly temporally and spatially restricted nature of its expression pattern. Furthermore, *CVP2* acts early in defining those cells that will participate in procambial strand formation. Identification of upstream regulators and downstream targets will aid in elucidating the role of *CVP2*-mediated IP_3 signaling in venation patterns.

METHODS

Plant Materials and Growth Conditions

cvp2-1, *cvp2-2*, and *cvp2-3* were identified from an ethyl methanesulfonate–mutagenized population (Carland et al., 1999) of the Columbia ecotype (Col). *cvp2-4*, *cvp2-5*, and *cvp2-6* were identified in a diepoxybutane-mutagenized population of Col (N. Clay and T. Nelson, unpublished data). The *cvp2-1* allele was used in all studies unless otherwise noted. DR5:GUS and Athb8:GUS are single-copy transgenes in Col. Only plants homozygous for the reporter gene construct and *cvp2-1* were used in this study. Seed was surface sterilized and plated on MS media (Sigma, St. Louis, MO)/0.75% agar supplemented with 1% sucrose and B5 vitamins, pH 5.7. After a 2 to 3 d of cold treatment in the dark, the plates were transferred to growth chambers with continuous light at 21°C. Seven-day-old light-grown seedlings were transplanted to 2:1 Metro Mix 200:vermiculite and grown with similar light and temperature conditions. To test *cvp2* response to ABA, seed was plated on media containing 0, 0.5, 1.0, and 2.0 μM ABA, cold treated (4°C) for 3 d, and transferred to light. Seed germination was scored at 24-h intervals for 6 d. Seed was considered germinated when the radicle had fully emerged from the seed coat. *cvp2* response assays to NaCl and mannitol were conducted as reported (Xiong et al., 2001). For root inhibition studies, wild-type and *cvp2* seeds were grown on MS media for 4 d and transferred to media with and without 10 μM ABA. Root growth in the presence of ABA was measured after 4 d of vertical growth and expressed as a percentage of root growth in the absence of hormone. Experiments were done in triplicate.

Histology and GUS Staining

Foliar tissue was cleared and prepared for photography as previously described (Carland et al., 1999). To visualize GUS staining, we used a staining solution composed of 100 mM phosphate buffer, pH 7.0, 1 mM EDTA, pH 8.0, 2 mM β-mercaptoethanol, 100 μg/mL of chloramphenicol, 0.01% Triton X-100, 2 mM 5-bromo-4-chloro-3-indoyl-β-D-glucuronide, and 5 mM potassium ferricyanide and ferrocyanide. Embryos were dissected from ovules before staining to ensure an even distribution of substrate. After vacuum infiltration of GUS stain, samples were placed at 37°C for 4 to 6 h. GUS stain was replaced with fixative (3:1 ethanol:acetic acid) and placed at 4°C overnight. Specimens were dehydrated with 70 and 100% ethanol at 4°C, cleared in 10% NaOH at 37°C for 3 to 4 h, and mounted in 50% glycerol. Specimens were viewed shortly after mounting and photographed with a Zeiss Axiophot microscope (Jena, Germany) using dark-field and Nomarski optics. Following this method, there was minimal GUS diffusion.

Positional Cloning of *CVP2*

cvp2-1 (Col) was crossed to Landsberg *erecta* to generate a large mapping population ($n = 804$ plants). Plants were scored at the seedling stage by removal of a cotyledon that had been cleared in fixative. Seedlings were then transplanted to soil and allowed to self-fertilize, yielding F3 seed. F3 seed was scored by clearing ~30 seedlings from each F2 plant. DNA was isolated as described by Carland et al. (2002),

and PCR was performed with standard conditions. Novel polymorphic markers were identified by three methods. (1) A gene on the restriction fragment length polymorphism map in the vicinity of *CVP2* was used as a marker on genomic DNA gel blots or converted to a PCR-based polymorphic marker. (2) As BAC DNA sequence became available on the Arabidopsis Information Resource Web site (http://www.arabidopsis.org/), small segments of DNA were amplified from Col and Landsberg *erecta* ecotypes and sequenced. Sequences were analyzed for base pair changes that could be converted to a polymorphism by cleaved-amplified polymorphic sequence or derived cleaved-amplified polymorphic sequence methods. (3) BAC DNA sequences were scanned by eye for regions of low complexity (i.e., AT-rich regions) that were tested for use as small nucleotide polymorphisms. Three libraries were screened for *cvp2* complementing clones. Screening of the TAC library was performed as previously described (Carland et al., 2002). A binary cosmid chapter library (Schulz et al., 1994) was screened with amplified PCR products from the *CVP2* spanning region. Secondary and tertiary screens were conducted on positive chapters until a single clone had been identified. Restriction enzyme and sequence analysis confirmed the map position of the cosmid. Single clones were electroporated into *Agrobacterium tumefaciens*, and positive clones were chosen as small tetracycline (2 μg/mL) resistant colonies (larger colonies were identified as spontaneous mutants). A third library was prepared from Sau3A1 partially digested BAC F3F20 DNA on which *CVP2* was thought to reside. Size-selected (8 to 12 kb) DNA was isolated by low melt agarose followed by β-agarase digestion according to the manufacturer's instructions (New England Biolabs, Beverly, MA) and ligated to *Bam*H1-digested pCAMBIA 2300 (CAMBIA, Canberra, Australia). Map positions of clones were determined by fingerprinting methods and confirmed by DNA sequence of clone ends. After electroporation of clones into *A. tumefaciens*, they were introduced into *Arabidopsis thaliana* genotypes using the floral dip method (Clough and Bent, 1998).

Plasmid Constructions

A *CVP2* genomic clone was isolated from BAC T25N20 DNA by PCR using the primers T12.9 (5′-GGTTTTGGCAATTTGTATCCC-3′) and T12.1 (5′-GTCCTAATCTGTCGGTTTGGTG-3′) and cloned into pCR2.1-TOPO vector (Invitrogen, Carlsbad, CA) to generate the construct p1791. p1791 was digested with *Eco*RI and ligated to pCAMBIA2300 to construct p1851. Fifty-seven independent transformants of p1851 in *cvp2* were assessed for complementation of the vascular patterning defect. Approximately 15% did not show complementation, presumably because of position effects, and were not analyzed further. CVP2:GUS construct was designed by amplifying Col DNA with T12.9 and T12.10 (5′-GCTTTTAAATTCCATGAAGATGGGC-3′) and cloning the amplified product into pCR2.1. This construct (p1751) was digested with *Bam*H1 and *Xba*I and ligated to pBI101 (Clontech, Palo Alto, CA) that had been digested with *Xba*I and *Bam*HI. Multiple independent lines were analyzed for CVP2:GUS expression and showed similar expression profiles. A line with a single transgene was selected for detailed analysis. Overexpression of a genomic clone of *CVP2* that spanned the coding region was constructed by amplifying this region with the primers T12-21 (5′-GAAGATCTTCGCCCATCTTCATGGAATTTAAAAGC-3′) and T12-22 (5′-GAACTAGTCCGCGAATTTGTGTGTTTCTAG-3′) that were engineered with *Bgl*II and *Spe*I sites, respectively. After digestion, the DNA was ligated to *Xba*I- and *Bam*HI-digested pZP35 (Hadjukiewicz et al., 1994) DNA to generate the construct p1972. We experienced difficulty in amplifying *CVP2* cDNA from several different tissue sources using RT-PCR. To isolate *CVP2* cDNA, RNA was prepared from Col/p1972 seedlings for use as template RNA, with random hexamers as downstream primers. A first round of RT-PCR using several primer pairs did not yield a product; therefore, a second round of PCR was performed using the nested primers T12-24 (5′- GAATTTCTGAAATGAAGCTGGC-3′) and T12-13 (5′-CTAGAAGAAGCTGAGCTCGG-3′). This PCR yielded a single product of ~1.8 kb whose identity was confirmed with sequence analysis. *CVP2* cDNA was subcloned into a plant transformation vector as described above.

All PCR-based clones were sequenced for verification.

IP_3 Assays

IP_3 assays were conducted using the radioreceptor method (Amersham TRK1000; Piscataway, NJ) according to the manufacturer's instructions with several modifications.

Briefly, 2 g of 8-d-old media-grown seedlings were ground in liquid nitrogen. Then, 0.4 mL of 20% perchloric acid was added for extraction of IP_3 from the cells. Samples were placed on ice for 20 min and sonicated for 15 s with a duty cycle of 50 at a medium setting. After centrifugation, the supernatant was titrated to pH 7.5. Samples were centrifuged to remove precipitate, and extracts were frozen until use. Counts were assayed using a scintillation counter programmed to measure H^3. Following the manufacturer's suggestions, all controls were performed, and a dilution series was conducted to ensure no inhibitors were present. Recovery yields were also measured.

Sequence data from this article have been deposited with the GenBank/EMBL data libraries under accession numbers AA037964, AAB68647, CAB42372, CAB07490, ACC44428, and Q14642.

ACKNOWLEDGMENTS

We would like to thank Hsu-Liang Hsieh and Genki Suzuki (formerly of Yale University) for advice in library construction, Nicole Kho for providing *cvp2-4*, *cvp2-5*, and *cvp2-6*, members of the laboratory of Timothy Nelson for valuable discussions, and Neil McHale (Connecticut Agricultural Experiment Station) for critical review of the manuscript. We are grateful to Jane Murfett and Tom Guilfoyle (University of Missouri, Columbia) and Nancy Dengler (University of Toronto) for providing DR5:GUS and Athb8:GUS transgenic lines, respectively. We acknowledge the ABRC for providing TAC and BAC clones. This research was supported by National Science Foundation Grant IBN-0110730 to T.N.

Received January 16, 2004; accepted February 24, 2004.

REFERENCES

Allen, G.J., Chu, S.P., Harrington, C.L., Schumacher, K., Hoffmann, T., Tang, Y.Y., Grill, E., and Schroeder, J.I. (2001). A defined range of guard cell calcium oscillation parameters encodes stomatal movements. Nature **411,** 1053–1057.

Baima, S., Nobili, F., Sessa, G., Lucchetti, S., Ruberti, I., and Morelli, G. (1995). The expression of the Athb-8 homeobox gene is restricted to provascular cells in Arabidopsis thaliana. Development **121,** 4171–4182.

Berdy, S.E., Kudla, J., Gruissem, W., and Gillaspy, G.E. (2001). Molecular characterization of At5PTase1, an inositol phosphatase capable of terminating inositol trisphosphate signaling. Plant Physiol. **126,** 801–810.

Berleth, T., and Jurgens, G. (1993). The role of the *monopteros* gene in organizing the basal body region of the *Arabidopsis* embryo. Development **118,** 575–587.

Berridge, M.J. (1993). Inositol trisphosphate and calcium signalling. Nature **361,** 315–325.

Berridge, M.J. (1995). Calcium signalling and cell proliferation. Bioessays **17,** 491–500.

Berridge, M.J., Bootman, M.D., and Roderick, H.L. (2003). Calcium signalling: Dynamics, homeostasis and remodelling. Nat. Rev. Mol. Cell Biol. **4,** 517–529.

Bui, Y.K., and Sternberg, P.W. (2002). *Caenorhabditis elegans* inositol 5-phosphatase homolog negatively regulates inositol 1,4,5-triphosphate signaling in ovulation. Mol. Biol. Cell **13,** 1641–1651.

Burnette, R.N., Gunesekera, B.M., and Gillaspy, G.E. (2003). An Arabidopsis inositol 5-phosphatase gain-of-function alters abscisic acid signaling. Plant Physiol. **132,** 1011–1019.

Busch, M., Mayer, U., and Jurgens, G. (1996). Molecular analysis of the Arabidopsis pattern formation of gene *GNOM*: Gene structure and intragenic complementation. Mol. Gen. Genet. **250,** 681–691.

Candela, H., Martinez-Laborda, A., and Micol, J.L. (1999). Venation pattern formation in *Arabidopsis thaliana* vegetative leaves. Dev. Biol. **205,** 205–216.

Carland, F.M., Berg, B.L., FitzGerald, J.N., Jinamornphongs, S., Nelson, T., and Keith, B. (1999). Genetic regulation of vascular tissue patterning in Arabidopsis. Plant Cell **11,** 2123–2137.

Carland, F.M., Fujioka, S., Takatsuto, S., Yoshida, S., and Nelson, T. (2002). The identification of *CVP1* reveals a role for sterols in vascular patterning. Plant Cell **14,** 2045–2058.

Carland, F.M., and McHale, N.A. (1996). *LOP1*: A gene involved in auxin transport and vascular patterning in Arabidopsis. Development **122,** 1811–1819.

Casson, S.A., Chilley, P.M., Topping, J.F., Evans, I.M., Souter, M.A., and Lindsey, K. (2002). The *POLARIS* gene of Arabidopsis encodes a predicted peptide required for correct root growth and leaf vascular patterning. Plant Cell **14,** 1705–1721.

Choe, S., Noguchi, T., Fujioka, S., Takatsuto, S., Tissier, C.P., Gregory, B.D., Ross, A.S., Tanaka, A., Yoshida, S., Tax, F.E., and Feldmann, K.A. (1999). The Arabidopsis dwf7/ste1 mutant is defective in the delta7 sterol C-5 desaturation step leading to brassinosteroid biosynthesis. Plant Cell **11,** 207–221.

Clay, N.K., and Nelson, T. (2002). VH1, a provascular cell-specific receptor kinase that influences leaf cell patterns in Arabidopsis. Plant Cell **14,** 2707–2722.

Clough, S.J., and Bent, A.F. (1998). Floral dip: A simplified method for Agrobacterium-mediated transformation of Arabidopsis thaliana. Plant J. **16,** 735–743.

Cnops, G., Wang, X., Linstead, P., Van Montagu, M., Van Lijsebettens, M., and Dolan, L. (2000). *Tornado1* and *tornado2* are required for the specification of radial and circumferential pattern in the Arabidopsis root. Development **127,** 3385–3394.

Connolly, T.M., Bross, T.E., and Majerus, P.W. (1985). Isolation of a phosphomonoesterase from human platelets that specifically hydrolyzes the 5-phosphate of inositol 1,4,5-trisphosphate. J. Biol. Chem. **260,** 7868–7874.

Cutler, S., Ghassemian, M., Bonetta, D., Cooney, S., and McCourt, P. (1996). A protein farnesyl transferase involved in abscisic acid signal transduction in Arabidopsis. Science **273,** 1239–1241.

Dengler, N. (2001). Regulation of vascular development. J. Plant Growth Regul. **20,** 1–13.

Dengler, N., and Kang, J. (2001). Vascular patterning and leaf shape. Curr. Opin. Plant Biol. **4,** 50–56.

Deyholos, M.K., Cordner, G., Beebe, D., and Sieburth, L.E. (2000). The *SCARFACE* gene is required for cotyledon and leaf vein patterning. Development **127,** 3205–3213.

Diener, A.C., Li, H., Zhou, W., Whoriskey, W.J., Nes, W.D., and Fink, G.R. (2000). *STEROL METHYLTRANSFERASE 1* controls the level of cholesterol in plants. Plant Cell **12,** 853–870.

Dlakic, M. (2000). Functionally unrelated signalling proteins contain a fold similar to Mg^{2+}-dependent endonucleases. Trends Biochem. Sci. **25,** 272–273.

Ducibella, T., Huneau, D., Angelichio, E., Xu, Z., Schultz, R.M., Kopf, G.S., Fissore, R., Madoux, S., and Ozil, J.P. (2002). Egg-to-embryo transition is driven by differential responses to Ca^{2+} oscillation number. Dev. Biol. **250,** 280–291.

Ettlinger, C., and Lehle, L. (1988). Auxin induces rapid changes in phosphatidylinositol metabolites. Nature **331,** 176–178.

Galweiler, L., Guan, C., Muller, A., Wisman, E., Mendgen, K., Yephremov, A., and Palme, K. (1998). Regulation of polar auxin transport by AtPIN1 in Arabidopsis vascular tissue. Science **282,** 2226–2230.

Gosti, F., Beaudoin, N., Serizet, C., Webb, A.A., Vartanian, N., and Giraudat, J. (1999). ABI1 protein phosphatase 2C is a negative regulator of abscisic acid signaling. Plant Cell **11,** 1897–1910.

Grebe, M., Xu, J., Mobius, W., Ueda, T., Nakano, A., Geuze, H.J., Rook, M.B., and Scheres, B. (2003). Arabidopsis sterol endocytosis involves actin-mediated trafficking via ARA6-positive early endosomes. Curr. Biol. **13,** 1378–1387.

Hadjukiewicz, P., Svab, Z., and Maliga, P. (1994). The small, versatile pZP family of Agrobacterium binary vectors for plant transformation. Plant Mol. Biol. **25,** 989–994.

Hamann, T., Benkova, E., Baurle, I., Kientz, M., and Jurgens, G. (2002). The Arabidopsis *BODENLOS* gene encodes an auxin response protein inhibiting *MONOPTEROS*-mediated embryo patterning. Genes Dev. **16,** 1610–1615.

Hamann, T., Mayer, U., and Jurgens, G. (1999). The auxin-insensitive bodenlos mutation affects primary root formation and apical-basal patterning in the Arabidopsis embryo. Development **126,** 1387–1395.

Hardtke, C.S., and Berleth, T. (1998). The Arabidopsis gene *MONOPTEROS* encodes a transcription factor mediating embryo axis formation and vascular development. EMBO J. **17,** 1405–1411.

Hobbie, L., McGovern, M., Hurwitz, L.R., Pierro, A., Liu, N.Y., Bandyopadhyay, A., and Estelle, M. (2000). The *axr6* mutants of Arabidopsis thaliana define a gene involved in auxin response and early development. Development **127,** 23–32.

Inoue, T., Higuchi, M., Hashimoto, Y., Seki, M., Kobayashi, M., Kato, T., Tabata, S., Shinozaki, K., and Kakimoto, T. (2001). Identification of CRE1 as a cytokinin receptor from Arabidopsis. Nature **409,** 1060–1063.

Jang, J.C., Fujioka, S., Tasaka, M., Seto, H., Takatsuto, S., Ishii, A., Aida, M., Yoshida, S., and Sheen, J. (2000). A critical role of sterols in embryonic patterning and meristem programming revealed by the *fackel* mutants of Arabidopsis thaliana. Genes Dev. **14,** 1485–1497.

Jung, J.Y., Kim, Y.W., Kwak, J.M., Hwang, J.U., Young, J., Schroeder, J.I., Hwang, I., and Lee, Y. (2002). Phosphatidylinositol 3- and 4-phosphate are required for normal stomatal movements. Plant Cell **14,** 2399–2412.

Kang, J., and Dengler, N. (2002). Cell cycling frequency and expression of the homeobox gene *ATHB-8* during leaf vein development in Arabidopsis. Planta **216,** 212–219.

Kinsman, E.A., and Pyke, K.A. (1998). Bundle sheath cells and cell-specific plastid development in Arabidopsis leaves. Development **125,** 1815–1822.

Kwak, J.M., Moon, J.H., Murata, Y., Kuchitsu, K., Leonhardt, N., DeLong, A., and Schroeder, J.I. (2002). Disruption of a guard cell-expressed protein phosphatase 2A regulatory subunit, RCN1, confers abscisic acid insensitivity in Arabidopsis. Plant Cell **14,** 2849–2861.

Liu, Y.G., Shirano, Y., Fukaki, H., Yanai, Y., Tasaka, M., Tabata, S., and Shibata, D. (1999). Complementation of plant mutants with large genomic DNA fragments by a transformation-competent artificial chromosome vector accelerates positional cloning. Proc. Natl. Acad. Sci. USA **96,** 6535–6540.

Lois, L.M., Lima, C.D., and Chua, N.H. (2003). Small ubiquitin-like modifier modulates abscisic acid signaling in Arabidopsis. Plant Cell **15,** 1347–1359.

Mahonen, A.P., Bonke, M., Kauppinen, L., Riikonen, M., Benfey, P.N., and Helariutta, Y. (2000). A novel two-component hybrid molecule regulates vascular morphogenesis of the Arabidopsis root. Genes Dev. **14,** 2938–2943.

Majerus, P.W., Kisseleva, M.V., and Norris, F.A. (1999). The role of phosphatases in inositol signaling reactions. J. Biol. Chem. **274,** 10669–10672.

Mattsson, J., Ckurshumova, W., and Berleth, T. (2003). Auxin signaling in Arabidopsis leaf vascular development. Plant Physiol. **131,** 1327–1339.

Mattsson, J., Sung, Z.R., and Berleth, T. (1999). Responses of plant vascular systems to auxin transport inhibition. Development **126,** 2979–2991.

Matzaris, M., O'Malley, C.J., Badger, A., Speed, C.J., Bird, P.I., and Mitchell, C.A. (1998). Distinct membrane and cytosolic forms of inositol polyphosphate 5-phosphatase II. Efficient membrane localization requires two discrete domains. J. Biol. Chem. **273,** 8256–8267.

Meinhardt, H. (1996). Models of biological pattern formation: Common mechanism in plant and animal development. Int. J. Dev. Biol. **40,** 123–134.

Murguia, J.R., Belles, J.M., and Serrano, R. (1995). A salt-sensitive 3′(2'),5′-bisphosphate nucleotidase involved in sulfate activation. Science **267,** 232–234.

Nelson, T., and Dengler, N. (1997). Leaf vascular pattern formation. Plant Cell **9,** 1121–1135.

Pei, Z.M., Ghassemian, M., Kwak, C.M., McCourt, P., and Schroeder, J.I. (1998). Role of farnesyltransferase in ABA regulation of guard cell anion channels and plant water loss. Science **282,** 287–290.

Perera, I.Y., Love, J., Heilmann, I., Thompson, W.F., and Boss, W.F. (2002). Up-regulation of phosphoinositide metabolism in tobacco cells constitutively expressing the human type I inositol polyphosphate 5-phosphatase. Plant Physiol. **129,** 1795–1806.

Przemeck, G.K., Mattsson, J., Hardtke, C.S., Sung, Z.R., and Berleth, T. (1996). Studies on the role of the Arabidopsis gene MONOPTEROS in vascular development and plant cell axialization. Planta **200,** 229–237.

Quintero, F.J., Garciadeblas, B., and Rodriguez-Navarro, A. (1996). The SAL1 gene of Arabidopsis, encoding an enzyme with 3′(2'),5′-bisphosphate nucleotidase and inositol polyphosphate 1-phosphatase activities, increases salt tolerance in yeast. Plant Cell **8,** 529–537.

Roth-Nebelsick, A., Uhl, D., Mosbrugger, V., and Kerp, H. (2001). Evolution and function of leaf venation architecture: A review. Ann. Bot. **87,** 553–566.

Sabatini, S., Beis, D., Wolkenfelt, H., Murfett, J., Guilfoyle, T., Malamy, J., Benfey, P., Leyser, O., Bechtold, N., Weisbeek, P., and Scheres, B. (1999). An auxin-dependent distal organizer of pattern and polarity in the Arabidopsis root. Cell **99,** 463–472.

Sachs, T. (1991). Cell polarity and tissue patterning in plants. Dev. Suppl. **1,** 83–93.

Sanchez, J.P., and Chua, N.H. (2001). Arabidopsis PLC1 is required for secondary responses to abscisic acid signals. Plant Cell **13,** 1143–1154.

Scarpella, E., Rueb, S., and Meijer, A.H. (2003). The *RADICLELESS1* gene is required for vascular pattern formation in rice. Development **130,** 645–658.

Schrick, K., Mayer, U., Horrichs, A., Kuhnt, C., Bellini, C., Dangl, J., Schmidt, J., and Jurgens, G. (2000). *FACKEL* is a sterol C-14 reductase required for organized cell division and expansion in Arabidopsis embryogenesis. Genes Dev. **14,** 1471–1484.

Schrick, K., Mayer, U., Martin, G., Bellini, C., Kuhnt, C., Schmidt, J., and Jurgens, G. (2002). Interactions between sterol biosynthesis genes in embryonic development of Arabidopsis. Plant J. **31,** 61–73.

Schulz, B., Bennett, M., Dilkes, B., and Feldmann, K. (1994). T-DNA tagging in Arabidopsis: Cloning by gene disruption. In Plant Molecular Biology Manual K3. (Belgium: Kluwer Academic Publishers), pp. 1–14.

Shevell, D.E., Leu, W.M., Gillmor, C.S., Xia, G., Feldmann, K.A., and Chua, N.H. (1994). *EMB30* is essential for normal cell division, cell expansion, and cell adhesion in Arabidopsis and encodes a protein that has similarity to Sec7. Cell **77,** 1051–1062.

Sieburth, L.E. (1999). Auxin is required for leaf vein pattern in Arabidopsis. Plant Physiol. **121,** 1179–1190.

Souter, M., Topping, J., Pullen, M., Friml, J., Palme, K., Hackett, R., Grierson, D., and Lindsey, K. (2002). *hydra* Mutants of Arabidopsis are defective in sterol profiles and auxin and ethylene signaling. Plant Cell **14,** 1017–1031.

Speed, C.J., Little, P.J., Hayman, J.A., and Mitchell, C.A. (1996). Underexpression of the 43 kDa inositol polyphosphate 5-phosphatase is associated with cellular transformation. EMBO J. **15,** 4852–4861.

Speed, C.J., Neylon, C.B., Little, P.J., and Mitchell, C.A. (1999). Underexpression of the 43 kDa inositol polyphosphate 5-phosphatase is associated with spontaneous calcium oscillations and enhanced calcium responses following endothelin-1 stimulation. J. Cell Sci. **112,** 669–679.

Steynen, Q.J., and Schultz, E.A. (2003). The FORKED genes are essential for distal vein meeting in Arabidopsis. Development **130,** 4695–4708.

Szekeres, M., Nemeth, K., Koncz-Kalman, Z., Mathur, J., Kauschmann, A., Altmann, T., Redei, G.P., Nagy, F., Schell, J., and Koncz, C. (1996). Brassinosteroids rescue the deficiency of CYP90, a cytochrome P450, controlling cell elongation and deetiolation in Arabidopsis. Cell **85,** 171–182.

Telfer, A., and Poethig, R.S. (1994). Leaf development in *Arabidopsis*. In Arabidopsis, E.M. Meyerowitz and C.R. Somerville, eds (Cold Spring Harbor, NY: Cold Spring Harbor Laboratory Press), pp. 379–401.

Tsujishita, Y., Guo, S., Stolz, L.E., York, J.D., and Hurley, J.H. (2001). Specificity determinants in phosphoinositide dephosphorylation: Crystal structure of an archetypal inositol polyphosphate 5-phosphatase. Cell **105,** 379–389.

Ulmasov, T., Murfett, J., Hagen, G., and Guilfoyle, T.J. (1997). Aux/IAA proteins repress expression of reporter genes containing natural and highly active synthetic auxin response elements. Plant Cell **9,** 1963–1971.

Willemsen, V., Friml, J., Grebe, M., van den Toorn, A., Palme, K., and Scheres, B. (2003). Cell polarity and PIN protein positioning in Arabidopsis require *STEROL METHYLTRANSFERASE1* function. Plant Cell **15,** 612–625.

Xiong, L., Lee, B., Ishitani, M., Lee, H., Zhang, C., and Zhu, J.K. (2001). *FIERY1* encoding an inositol polyphosphate 1-phosphatase is a negative regulator of abscisic acid and stress signaling in Arabidopsis. Genes Dev. **15,** 1971–1984.